Journal of Atmospheric and Solar–Terrestrial Physics 285 (2026) 106877

Contents lists available at ScienceDirect

Journal of Atmospheric and Solar-Terrestrial Physics

journal homepage: www.elsevier.com/locate/jastp

Research Paper

Long-term characterisation and discrimination of aerosol types across Africa using AERONET observations (1998–2024)

Yonah Situma [a], John W. Makokha [a], Peter N. Khakina [a], Geoffrey W. Khamala [b], Kanike Raghavendra Kumar [c,*], Richard Boiyo [d,e]

[a] Department of Science, Technology and Engineering, Kibabii University, P.O. BOX 1699, Bungoma, 50200, Kenya
[b] Department of Renewable Energy and Technology, Turkana University College, P.O. BOX 69, Lodwar, 30500, Kenya
[c] Department of Engineering Physics, College of Engineering, Koneru Lakshmaiah Education Foundation (KLEF), Vaddeswaram, Guntur, Andhra Pradesh, 522302, India
[d] Department of Physical Sciences, Meru University of Science and Technology, P.O. BOX 972, Meru, 60200, Kenya
[e] Department of Environment, Water, Energy and Resources, County Government of Vihiga, Maragoli, Kenya

ARTICLE INFO

Keywords:
Aerosol optical depth
Discrimination methods
Aerosol classification
AERONET
Africa

ABSTRACT

Accurate identification and classification of atmospheric aerosols remain a significant challenge across Africa, limiting the precise assessment of their climatic effects. This study presents a comprehensive analysis of aerosol characteristics and aerosol types using ground-based observations from twelve selected AErosol RObotic NETwork (AERONET) sites across Africa during 1998–2024. Key aerosol optical properties, including aerosol optical depth (AOD), Ångström exponent (AE), fine-mode fraction (FMF), and single scattering albedo (SSA), were examined to characterize their temporal variability and identify dominant aerosol types. A multivariate scattering-based classification approach was employed to improve aerosol discrimination. The results indicate that dust, biomass-burning, and urban/industrial aerosols are the predominant aerosol categories across the continent. Fine- and coarse-mode absorbing aerosols were particularly prevalent in rural tropical regions, highlighting the coexistence of natural and anthropogenic emission sources. Moreover, extensive biomass-burning activity in tropical Africa contributes substantially to regional aerosol loading and complexity. These findings provide valuable insights for improving the representation of aerosol processes in climate models and enhancing assessments of aerosol–climate interactions over Africa. The proposed multivariate framework advances aerosol classification and source attribution, supporting a better understanding of aerosol-related environmental and climatic impacts across the continent.

1. Introduction

Aerosols, defined as a suspension of fine solid particles or liquid droplets in the atmosphere, play a crucial role in atmospheric processes, climate dynamics, and public health (Seinfeld and Pandis, 1998; Tang et al., 2021; Chung et al., 2022; Althaf et al., 2025; Khamala et al., 2022, 2026). Their diverse origins, ranging from natural sources like volcanic eruptions and sea spray to anthropogenic activities such as industrial emissions and vehicular exhaust, create a complex mixture of particles with varying chemical compositions, sizes, and optical properties (Makokha et al., 2012; Ngaina et al., 2014; Al-Thani et al., 2018; Boiyo et al., 2018; Chaibou et al., 2020; Khamala and Makokha, 2025; Berhane et al., 2024, Berhane et al., 2025; Khamala et al., 2025). Therefore, distinguishing among these aerosol types is essential for understanding their specific impacts on climate forcing, air quality, and human health (Chen et al., 2017; Boiyo et al., 2019; Ranjan et al., 2024). The classification of aerosols is typically based on their physical and chemical characteristics. Physically, aerosols are categorised by size into coarse particles (diameters between 2.5 and 10 μm), fine particles (diameters less than 2.5 μm), and ultrafine particles (diameters less than 0.1 μm) (Holben et al., 1998; de Graaf et al., 2010; Ngaina and Mutai, 2013; Khamala *et al.*, 2025). These size distinctions are significant because they influence the lifetime of pollutant particles in the atmosphere, transport distances, and deposition sites within the human respiratory system, thereby affecting health outcomes (Gauderman et al., 2002; Yu et al., 2016; WHO, 2021; Khamala *et al.*, 2023).

Based on chemical composition, aerosols are composed of various substances, including sulfates, nitrates, organic carbon, black carbon,

* Corresponding author.
E-mail addresses: kanike.kumar@gmail.com, rkkanike@kluniversity.in (K.R. Kumar).

https://doi.org/10.1016/j.jastp.2026.106877
Received 20 February 2026; Received in revised form 15 June 2026; Accepted 18 June 2026
Available online 19 June 2026

sea salt, and mineral dust (). Each type has distinct sources and environmental effects. For instance, sulfates primarily originate from the oxidation of sulfur dioxide emitted by fossil fuel combustion and volcanic activity, contributing to atmospheric cooling by scattering sunlight (Seinfeld and Pandis, 1998; Tang et al., 2021). In contrast, black carbon, produced from incomplete combustion processes, absorbs sunlight, leading to atmospheric warming (Makokha et al., 2012; 2018; Chin et al., 2014; Khan et al., 2020; Khamala *et al.*, 2023; Althaf et al., 2024; Sangura et al., 2025). Aerosols can serve as cloud condensation nuclei or ice-nucleating particles, influencing cloud formation, properties, and precipitation processes (Makokha and Angeyo, 2013). Accurate classification of aerosol types enables researchers to better assess their indirect effects on climate through cloud modifications. Aerosol particles, such as dust and biological particles, have been identified as effective ice-nucleating particles, thereby affecting cloud glaciation processes and potentially altering precipitation patterns (Kanji et al., 2017; Makokha et al., 2024). The discrimination of aerosol types is crucial for understanding their direct effects on climate and health. This elucidates their roles in aerosol-cloud interactions (Mulago et al., 2024), particularly in Africa, since it carries the heaviest burden of the negative impacts of climate change.

Recent advancements in aerosol discrimination techniques have concentrated on enhancing the accuracy of differentiating between clouds and optically thick aerosols. For example, a study by Kim et al. (2022) explored the use of a three-wavelength approach to improve aerosol-cloud discrimination. By incorporating an additional wavelength channel at 1550 nm, the researchers boosted their ability to distinguish between aerosol and cloud particles, particularly in challenging scenarios where traditional methods may struggle. This approach capitalises on the distinct spectral signatures of aerosols and clouds across various wavelengths, providing a more robust classification framework. Another innovative method involves the rapid discrimination of aerosol particle shapes using light scattering techniques. Zhu et al. (2023) proposed an experimental setup capable of simultaneously measuring the intensity of angle-resolved light scattering, polarisation characteristics, and aerodynamic diameter of individual particles. By analysing the scattered light at two wavelengths and applying partial least squares discriminant analysis, the researchers established a predictive model to distinguish between spherical, rod-shaped, and other non-spherical particles. This technique provides a fast and effective way to characterize aerosol particle shapes, which is essential for understanding their behaviour and impacts in the atmosphere.

The impact of aerosols on both global and regional climates has been widely documented through numerous studies worldwide. This highlights the importance of conducting similar research focused on Africa, which would contribute to strengthening the existing knowledge on aerosol effects across the African continent. This study would also help reduce uncertainties in aerosol characterization by employing a multivariate approach whereby multiple aerosol optical parameters are used in discrimination with the intention of improving the accuracy of aerosol type discrimination, rather than relying on a single parameter. AOD-AE presents aerosol loading versus particle-size, FMF-SSA gives insight into fine mode fraction of aerosols plus absorption as well as scattering properties and lastly AE-FMF reinforces the dominance of particle size, thereby improving the aforementioned accuracy. The present paper has been structured in different sections as follows. The study area, data and methodology, as well as the objectives presented in Section 2, illustrate the description of AERONET sites, local meteorology, and the methodology adopted in analysing the data. Following this, the results and discussions are documented in Section 3, while the conclusions and recommendations (given in Section 4) summarise the key findings drawn from the present work and call for future scope of research.

2. Study area, meteorology, and instrumentation

2.1. Study domain and prevailing climate

Africa, the world's second-largest continent, spans a vast range of latitudes and longitudes, resulting in diverse climatic conditions. Geographically, the continent extends from approximately 37°21′ N latitude to 34°51′15″ S latitude, and from about 51°27′52″ E longitude to 17°33′22″ W longitude (Fig. 1). This expansive range places Africa between the Tropic of Cancer and the Tropic of Capricorn, encompassing both the Equator and the Prime Meridian. Consequently, Africa experiences a variety of climates, from equatorial rainforests to arid deserts (Khamala and Makokha, 2025). Africa's meteorology is characterised by a diverse array of climatic zones, weather patterns, and atmospheric phenomena, influenced by its vast geographical expanse and varied topography (Boiyo et al., 2017). The continent experiences a range of climates, from the arid deserts of the Sahara in the north to the tropical rainforests of the Congo Basin and the temperate regions in the south.

The northern half of Africa is dominated by the Sahara Desert, the world's largest hot desert, characterised by extremely low precipitation and high temperatures. South of the Sahara lies the Sahel, a semi-arid transition zone that experiences seasonal rainfall. Central Africa, particularly the Congo Basin, is home to dense tropical rainforests with high annual rainfall, while regions like the Horn of Africa and parts of Southern Africa exhibit arid and semi-arid climates (Aklesso et al., 2018; Berhane et al., 2025). The movement of the Intertropical Convergence Zone (ITCZ) plays a pivotal role in dictating rainfall patterns across the continent, leading to distinct wet and dry seasons in many regions. For instance, areas with a savannah climate, such as Ghana and Botswana, have a pronounced rainy season influenced by the northward and southward migration of the ITCZ (Khamala and Makokha, 2025). Although the study is limited to twelve AERONET sites, the selected stations were strategically distributed across northern, western, eastern, central, and southern Africa to capture major continental aerosol regimes, including dust, biomass burning, marine, and mixed aerosols. Consequently, the analysis emphasizes representative regional aerosol characteristics rather than exhaustive continental - scale spatial coverage.

2.2. Instrumentation and data

The AErosol RObotic NETwork (AERONET) is a globally distributed network of ground-based Sun-sky radiometers designed to monitor optical, microphysical, and radiative properties of aerosols. The primary instrument utilised in this network is the CIMEL Electronique (Model CE-318) sun-sky radiometer, which performs direct Sun measurements at multiple wavelengths, typically 340, 380, 440, 500, 675, 870, 940, and 1020 nm at an interval of 15 min. These measurements are instrumental in deriving key aerosol optical properties, including aerosol optical depth (AOD), Ångström exponent (AE), single scattering albedo (SSA), and fine mode fraction (FMF) (e.g., Holben et al., 1998; Kumar et al., 2018; Boiyo et al., 2018; Khan et al., 2019). A detailed list of AERONET sites located across Africa, along with their environmental type and data period, is shown in Table 1.

AOD quantifies the degree to which aerosols prevent the transmission of sunlight by absorption or scattering (Makokha et al., 2015; Kumar et al., 2017). It is a dimensionless parameter indicating the integrated columnar extinction of solar radiation due to aerosols from the Earth's surface to the top of the atmosphere. Higher AOD values correspond to more turbid atmospheric conditions. The spectral measurements of AOD are foundational for assessing aerosol loading in the atmosphere (Holben et al., 1998 and references therein). On the other hand, AE describes the wavelength dependency of AOD and serves as an indicator of aerosol particle size (Dubovik et al., 2002). It is calculated using the spectral AOD values and is inversely related to the aerodynamic diameter of particles. Higher AE values suggest the dominance

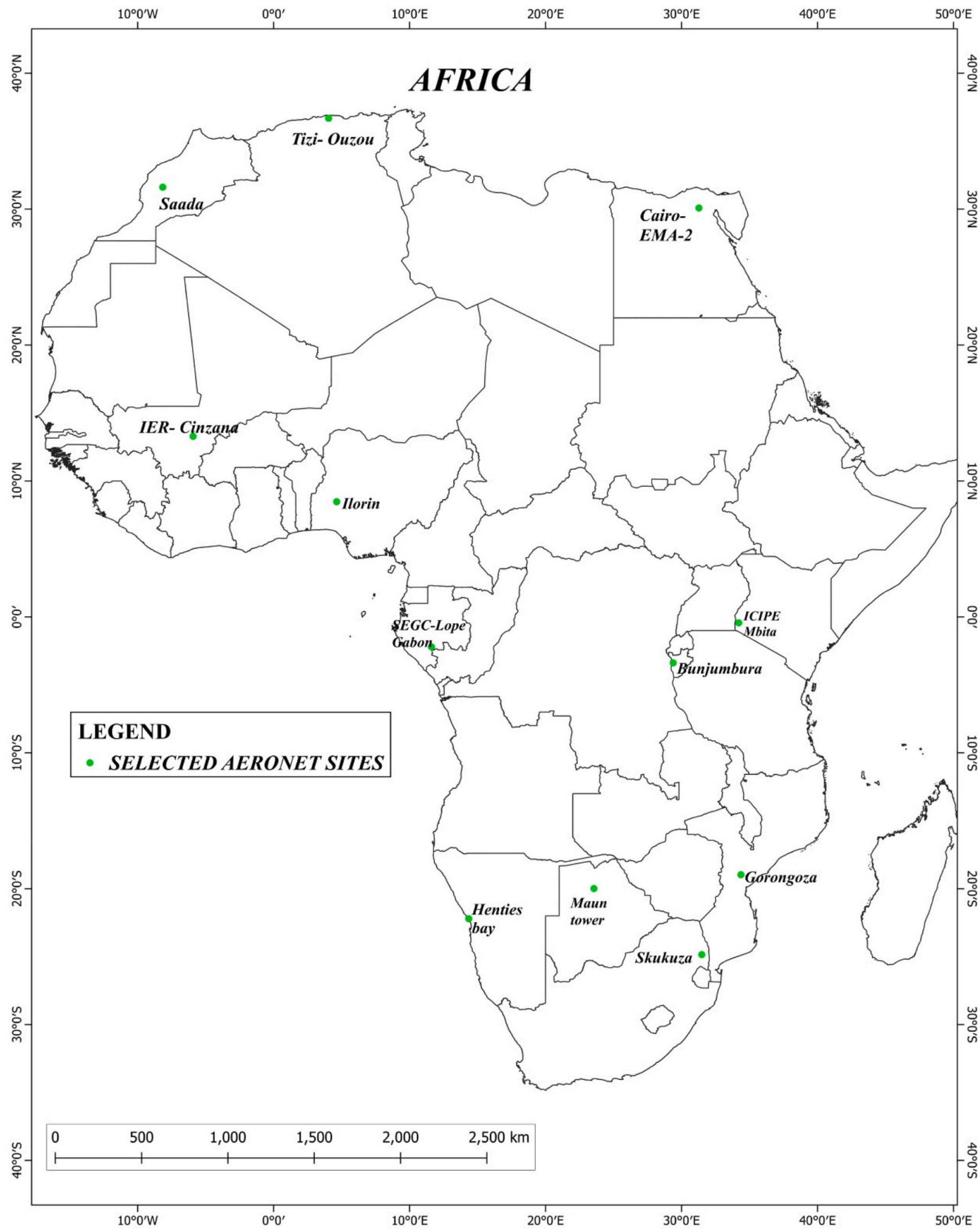

Fig. 1. Map of the study domain indicating the locations of the twelve AERONET sites (solid dots) over the African continent.

of fine-mode particles, while lower values indicate coarse-mode particles (Boiyo et al., 2019; Khamala et al., 2022). This parameter is essential for characterising aerosol types (Table 2) and their potential climatic impacts (Schuster et al., 2006). Further, SSA is the ratio of scattering to the total extinction (scattering plus absorption) coefficient by aerosols. It provides insight into the radiative properties of aerosols, distinguishing between predominantly scattering aerosols (SSA $\geq$0.90), moderately absorbing aerosols (SSA $\approx$ 0.85-0.90), and strongly absorbing aerosols (SSA $<$0.85). AERONET retrieves SSA by inverting sky radiance measurements, offering critical data for understanding aerosol radiative forcing (Dubovik et al., 2002; Gobbi et al., 2007; Toledano et al., 2007) (Table 3).

Lastly, FMF represents the proportion of AOD attributable to fine-mode particles relative to the total AOD. It is derived from the aerosol size distribution obtained through inversion algorithms applied to sky radiance data. FMF is particularly useful for distinguishing between fine and coarse aerosol contributions in various atmospheric conditions (O'Neill et al., 2001) (Table 3). These parameters, AOD, AE, SSA, and FMF, are pivotal in the characterisation of aerosols. They enable the discrimination of aerosol types, assessment of their optical properties, and evaluation of their climatic and environmental impacts. AERONET's standardised measurements and retrieval algorithms ensure consistent and reliable data across its global network, facilitating comprehensive aerosol studies (Holben et al., 1998). More details about the other deliverables, data precision, accuracy, and errors are described by several earlier authors (e.g., Boiyo et al., 2018).

Table 1
Geographical coordinates (latitude and longitude in degrees), altitude (in meters above sea level), environmental type, and duration of available AERONET observations for the selected sites across Africa. The negative values of latitude and longitude coordinates represent the coordinates along south and west, whereas the positive indicates north and east direction.

Country	AERONET site	Latitude	Longitude	Altitude	Type	Duration
Kenya	ICIPE-Mbita	−0.43	34.21	1152	Rural	11 (2006-2017)
South Africa	Skukuza	−24.99	31.59	265	Rural	23 (1998-2021)
Namibia	Henties Bay	−22.09	14.26	20	Marine	7 (2011-2018)
Zambia	Maun-Tower	−19.91	23.55	951	Industrial	19 (2000-2019)
Egypt	Cairo-EMA-2	30.08	31.29	70	Industrial	9 (2010-2019)
Morocco	Saada	31.62	−8.15	420	Rural	15 (2004-2019)
Mali	IER-Cinzana	13.28	−5.93	287	Rural	15 (2004-2019)
Mozambique	Gorongoza	−18.98	34.35	30	Rural	5 (2012-2017)
Algeria	Tizi-Ouzou	36.69	4.05	133	Industrial	5 (2012-2017)
Nigeria	Ilorin	8.48	4.64	400	Industrial	6 (2013-2019)
Burundi	Bujumbura	−3.38	29.38	863	Industrial	21 (1998-2019)
Gabon	SEGC-lope-Gabon	−2.21	11.60	280	Rural	4 (2014-2018)

Table 2
Threshold values employed for aerosol-type discrimination using AOD_{500} and $AE_{440-870}$ observations across African AERONET sites.

AOD_{500}	$AE_{440-870}$	Aerosol Type
<0.2	>1.0	Continental Clean Background (CCB)
<0.2	<0.9	Clean Marine (CMA)
>0.3	>1.0	Biomass Burning/Urban-Industrial (BUI)
>0.6	<0.7	Desert Dust (DDT)
Others	Others	Mixed (MXD)

Table 3
Threshold values of FMF_{500} nm and SSA_{440} nm used for aerosol-type discrimination by previous studies worldwide and adopted in the present study.

Type	FMF_{500nm}	SSA_{440nm}	Citation
BC	0.86	>0.85	Srivastava et al., 2014
PC	<0.48	>0.88	
Dust	<0.30	>0.92	
BC	0.5-1.00	0.84-0.97	Rupakheti et al., 2019
MXD	0.20-0.50	0.84-0.90	
Dust	0.10-0.40	0.90-0.95	
BC	>0.6	any range	Boiyo et al., 2019
PC	0.3-0.6	any range	
Dust	<0.3	any range	
BC	-	0.82-0.091	Bibi et al. (2016)
MXD	-	0.89-0.96	
Dust	-	0.88-.0.96	
BB	-	0.80-0.96	Shaheen et al., 2020
MXD	-	0.89-0.96	
Dust	-	0.89-0.95	
BB	0.6-0.9	0.84-0.86	
UI	0.4-0.6	0.96-0.98	
Dust	0.3-0.4	0.92-0.94	
BB	-	<0.85	Khan et al., 2021
MXD	-	0.85-0.90	
Dust	-	0.90-0.95	
BC	0.6-1	Any range	Present Study
MXD	0.3-0.6	Any range	
PC	<0.3	Any range	

2.3. Methodology

Aerosol discrimination involves distinguishing various aerosol types based on their optical and microphysical properties. In this study, aerosol classification was not performed using isolated single-parameter thresholds alone, but through an integrated multi-parameter discrimination framework that jointly evaluates aerosol optical depth (AOD), Ångström exponent (AE), fine mode fraction (FMF), and single scattering albedo (SSA) within a multidimensional aerosol feature space. The framework exploits the complementary physical sensitivities of these parameters to aerosol loading, particle size distribution, fine-mode dominance, and scattering–absorption characteristics, thereby improving aerosol regime separability beyond conventional bivariate threshold approaches. In this methodology, aerosol discrimination was performed using AOD, AE, SSA, and FMF within the specific threshold values (Tables 2 and 3). The threshold ranges presented in Tables 2 and 3, therefore, serve as physically guided reference boundaries for aerosol regime interpretation rather than strict deterministic classifiers.

These parameters are derived from satellite-based observations, ground-based measurements, and reanalysis datasets. For high temporal resolution, Moderate Resolution Imaging Spectroradiometer (MODIS) and Ozone Monitoring Instrument (OMI) provide global datasets of AOD, AE, SSA, and FMF data (Kumar et al., 2018). For ground-based measurements, AERONET data provide high-accuracy retrievals of aerosol properties such as SSA and FMF. Data from AERONET Level 2.0 (cloud-screened and quality-assured) are used in this study, derived for the period from 1998 to 2024. On the other hand, for reanalysis Products, MERRA-2 offers specific spatiotemporal coverage of AOD and FMF, complementing gaps in satellite and ground data. In the present analysis, each point in the figure represents a daily averaged value, derived from collocated AE and AOD observations corresponding to the same date. Thus, the dataset is based on temporally matched daily means rather than instantaneous measurements. Regarding data availability, the number of measurements varies with temporal aggregation. For sites with continuous observations, this corresponds to approximately one data point per day, about 30 per month, and up to 365 per year, subject to data quality screening and instrument availability.

These measurements are derived from the interaction between the incident solar radiation and matter. The amount of light detected by the photometers is compared with the solar radiation incoming, which would be observed in an aerosol-free (clean) atmosphere. From this comparison, the optical depth can be determined from the relation:

$$\tau = k(x)dx \tag{1}$$

where τ is the optical depth, k is the linear extinction coefficient product, and x is the distance. More precisely, if the extinction coefficient varies with distance, then the optical depth will be obtained by integrating the extinction coefficient with distance.

AE, on the other hand, provides size information about aerosols and is given as in Equation (2). Values > 1.0 suggest fine aerosols, while values < 0.5 indicate coarse aerosols such as dust or sea spray (Table 2).

$$\alpha = -\frac{d\ln\tau}{d\ln\lambda} \tag{2}$$

And Equation (3) for FMF, a direct measure of how much of the aerosol is fine particles (Table 3)

$$\mathrm{FMF} = \frac{\mathrm{AOD_F}}{\mathrm{AOD_T}} \tag{3}$$

Further, SSA reflects aerosol scattering efficiency (given in Equation (3)). Higher SSA (>0.9) indicates highly scattering aerosols, such as sulfates, whereas lower SSA (<0.85) suggests absorbing aerosols, such as black carbon (Bergstrom et al., 2022).

$$SSA = \frac{Q_{sca}}{Q_{sca} + Q_{abs}} = 1 + \frac{Q_{abs}}{Q_{ext}} \tag{4}$$

where Q_{abs} and Q_{sca} are the absorbed and scattered light, respectively.

Conventional univariate aerosol classification approaches, which rely on a single optical parameter such as AOD or AE, often fail to

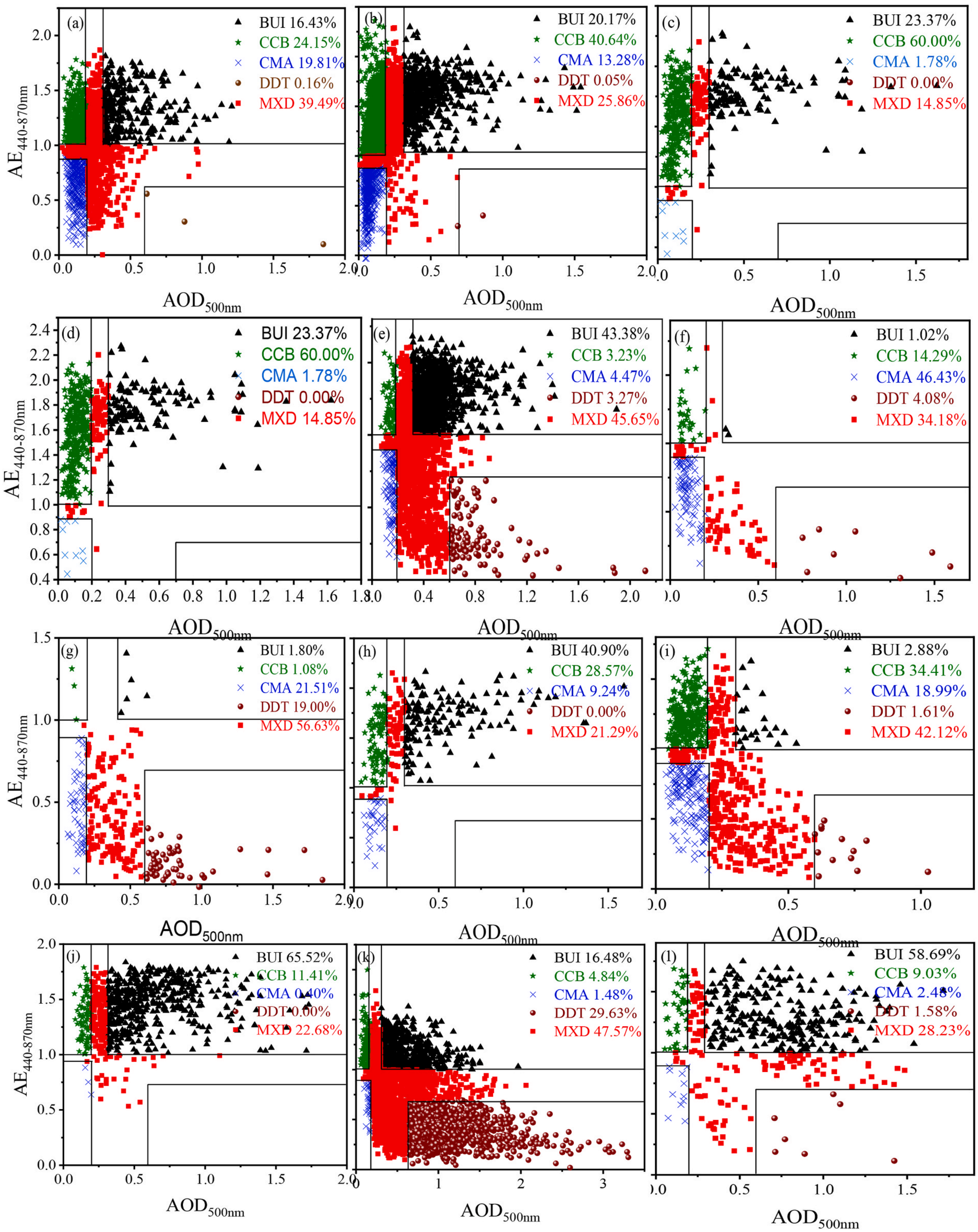

Fig. 2. Scatter plots of Ångström Exponent ($AE_{440-870}$) versus Aerosol Optical Depth (AOD_{500}) for selected AERONET sites across Africa. The panels (a–l) represent Mbita, Skukuza, Henties Bay, MaunTower, Cairo EMA-2, Saada, IER-Cinzana, Gorongosa, Tizi-Ouzou, Bujumbura, Ilorin, and SEGC-Lope-Gabon, respectively. These sites illustrate the variability in aerosol types across different regions, with threshold values indicated by vertical and horizontal reference lines.

adequately resolve the complexity of mixed and transitional aerosol regimes because individual parameters cannot simultaneously capture aerosol loading, particle size distribution, and radiative behavior (Li et al., 2023; Nicolae et al., 2018; Kumar et al., 2018). The integrated use of AE–AOD, FMF–AE, and SSA–FMF relationships in this study provides a physically constrained multivariate discrimination framework that jointly evaluates aerosol abundance, size dominance, fine-mode contribution, and scattering–absorption characteristics within a unified feature space. This combined approach reduces ambiguities commonly associated with traditional threshold-based methods and improves the separation of dust, biomass-burning, polluted continental, and mixed aerosols across climatically diverse African environments (Chaibou et al., 2020; Shikwambana and Sivakumar, 2018; Mishra et al., 2021; Shin et al., 2023). Recent studies have further demonstrated that multidimensional aerosol discrimination techniques outperform isolated parameter analyses in resolving aerosol heterogeneity, source mixing, and atmospheric aging processes (Wei et al., 2022). Furthermore, the simultaneous integration of ground-based AERONET observations with MODIS, CALIPSO, and MERRA-2 products enhanced the physical robustness and regional transferability of the discrimination framework beyond descriptive climatological interpretation. Consequently, the coupled parameter-space approach represents a methodological advancement over conventional univariate aerosol typing by enabling improved characterization of seasonal aerosol variability and aerosol–radiation interactions across Africa.

3. Results and discussion

3.1. AOD versus AE method

Fig. 2 presents scatter plots of AOD_{500} versus $AE_{440–870}$ for selected AERONET sites across Africa, where each data point represents a daily co-located average. The observed AE–AOD relationships provide a robust framework for aerosol classification. High AE values (>1.0) indicate the dominance of fine-mode aerosols, typically associated with biomass burning and urban-industrial emissions, whereas low AE values (<0.7) are characteristic of coarse-mode particles such as mineral dust (Eck et al., 2020; Chaibou et al., 2020).

At Mbita (Fig. 2a), mixed aerosols (MXD, 39.49%) constitute the dominant aerosol type, followed by biomass-burning aerosols (BU, 16.43%), reflecting a complex aerosol environment influenced by both local anthropogenic emissions and transported dust. Similar mixed aerosol conditions have been reported across Europe, where secondary aerosols and transported dust account for approximately 30–50% of aerosol occurrences under moderate AOD conditions (0.2–0.6) (Putaud et al., 2021; Sicard et al., 2020; Logothetis et al., 2020; Filonchyk et al., 2020). However, the larger variability in AE observed at Mbita suggests a stronger episodic influence of biomass-burning emissions compared with typical European environments.

Henties Bay (Fig. 2c), characterized by a predominance of cloud-condensed black carbon (CCB, 60.00%), reflects strong interactions between marine and continental air masses. Comparable coastal aerosol regimes have been documented in Southeast Asia, where marine aerosols mix with anthropogenic emissions, resulting in high fine-mode fractions (FMF >0.6) and AOD values ranging from approximately 0.3 to 0.8 (Nguyen et al., 2025; Mukhopadhyay et al., 2025). Nevertheless, aerosol conditions at Henties Bay appear to be more strongly influenced by natural marine sources, with relatively lower anthropogenic contributions than those observed in Southeast Asia.

IER-Cinzana (Fig. 2g) exhibits a pronounced dominance of dust aerosols (DDT, 19.90%), consistent with its location in the Sahel region. This observation agrees with studies conducted in India, Pakistan, and northern China, where dust aerosols contribute approximately 20–40% of total aerosol loading during dry seasons and are generally associated with low AE values (<0.5) and elevated AOD (>0.5) (Zhang et al., 2016; Yu et al., 2016). However, African dust systems originating from the Sahara are generally more persistent and spatially extensive, resulting in stronger regional radiative forcing effects.

The site represented in Fig. 2i, where biomass-burning aerosols (BU) account for 65.22% of observations, highlights the substantial influence of combustion-related emissions. This contribution exceeds the typical biomass-burning fractions reported across Europe (~10–30%) but is comparable to major biomass-burning hotspots in Southeast Asia and India, where contributions may reach 50–70% during peak burning seasons (Sicard et al., 2020; Nguyen et al., 2025). Such conditions are commonly associated with high AE values (>1.3) and enhanced concentrations of absorbing aerosols, which have important implications for radiative forcing and regional air quality.

A comparison of AERONET-derived aerosol classifications with satellite and reanalysis products, including MODIS, CALIPSO, and MERRA-2, demonstrates strong agreement in the spatial distribution and compositional variability of aerosols across Africa. MODIS AOD retrievals indicate elevated aerosol loading over the Sahara and Sahel regions (AOD >0.5), consistent with the dust-dominated conditions observed at IER-Cinzana. In contrast, moderate AOD values (~0.3–0.7) over central and southern Africa correspond closely with regions dominated by biomass-burning aerosols (Levy et al., 2013; Remer et al., 2020). Coastal locations such as Henties Bay exhibit lower AOD values (~0.2–0.4), reflecting the influence of marine aerosols, although MODIS retrievals may underestimate coarse-mode particles over bright desert surfaces (Hsu et al., 2023).

CALIPSO observations provide valuable vertical information, revealing elevated Saharan dust layers between 2 and 5 km altitude and lofted biomass-burning plumes between 1 and 3 km. These observations support the AE-based classification of coarse- and fine-mode aerosols, respectively (Winker et al., 2013). Furthermore, CALIPSO observations are consistent with MODIS-derived fine-mode AOD enhancements over West and Southern Africa during peak burning seasons, reflecting intense fire activity and reduced wet scavenging processes (Adesina et al., 2016; Remer et al., 2020).

Similarly, MERRA-2 reanalysis data indicate that carbonaceous aerosols, including black carbon and organic carbon, contribute approximately 50–80% of total AOD across major biomass-burning regions, further confirming the dominance of combustion-derived particles (Randles et al., 2017). The observed vertical mixing of dust and smoke layers also explains the high proportion of mixed aerosols (MXD) at Mbita, highlighting the importance of lidar observations for resolving aerosol layering and transport pathways. In addition, MERRA-2 attributes approximately 40–70% of total AOD over North and West Africa to dust aerosols, while biomass-burning aerosols contribute approximately 50–80% of AOD over equatorial and southern Africa (Randles et al., 2017; Buchard et al., 2017; Berhane et al., 2025). Coastal regions exhibit substantial sea-salt contributions (~30–60%), further supporting the influence of marine aerosol sources at coastal sites (Smirnov et al., 2019).

Although uncertainties remain due to limitations in MODIS surface reflectance retrievals, CALIPSO's narrow observational swath, and the model-dependent nature of MERRA-2 reanalysis products, the strong agreement among these independent datasets reinforces the reliability of the AE–AOD aerosol classification framework. Overall, the integration of ground-based observations, satellite measurements, and reanalysis products provides a comprehensive and robust characterization of aerosol regimes and their spatial variability across Africa.

3.2. FMF versus SSA

The FMF–SSA relationship illustrated in Fig. 3 provides a robust framework for aerosol classification across African AERONET sites by simultaneously constraining aerosol particle size and radiative properties. Comparison with satellite and reanalysis products, including MODIS, CALIPSO, and MERRA-2, reveals a consistent and complementary representation of aerosol regimes across the continent. High FMF

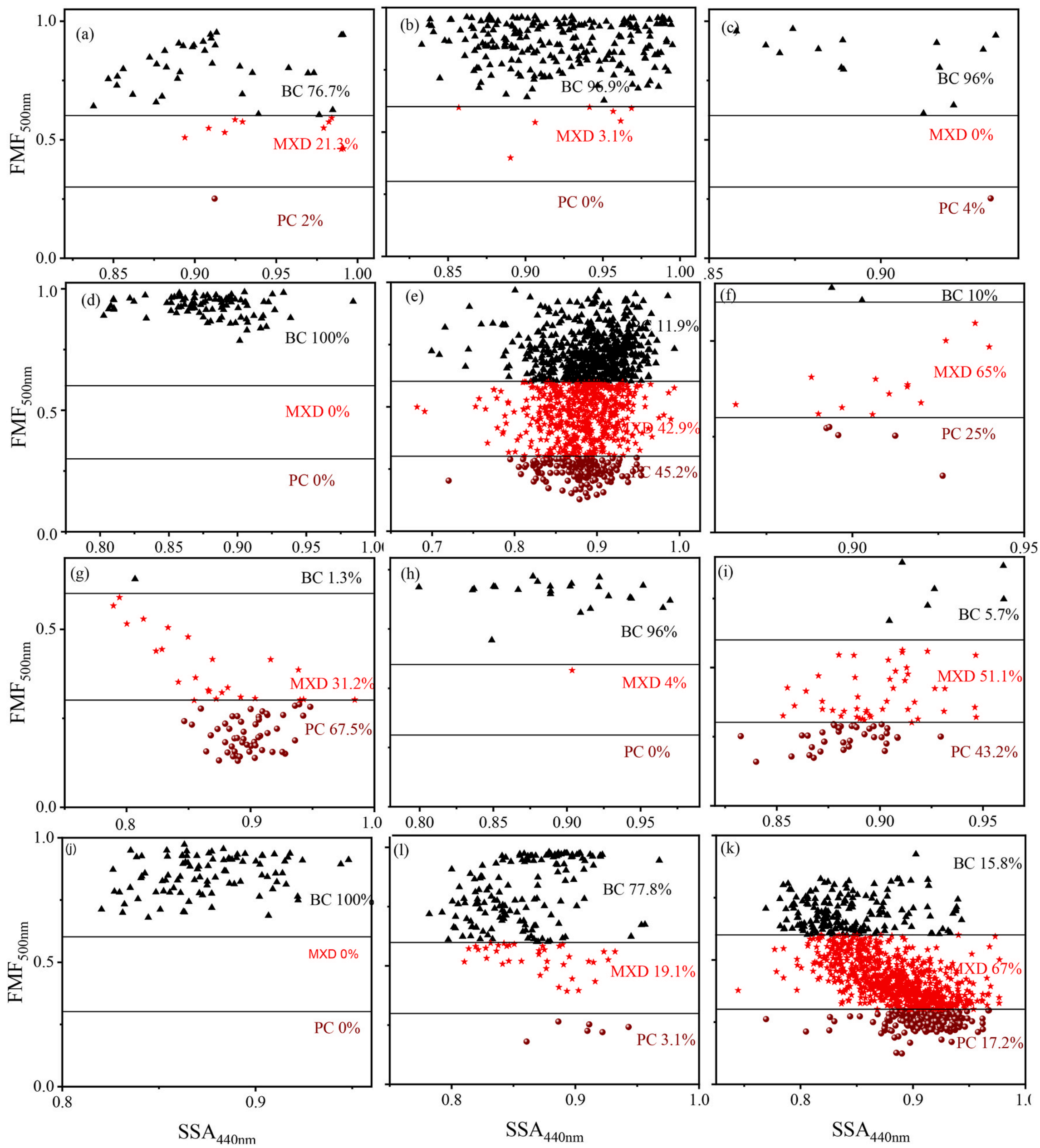

Fig. 3. Scatter plots of FMF_{500} versus SSA_{440} for selected AERONET sites across Africa, classified into different aerosol types. Black carbon (BC), mixed aerosols (MXD), and polluted continental (PC) regimes are shown, with corresponding percentage contributions indicating aerosol loading. Horizontal reference lines denote the threshold values used to separate aerosol regimes.

values (>0.6) coupled with low SSA values (∼0.80–0.90), indicative of fine-mode and strongly absorbing aerosols such as black carbon (BC), are typically associated with biomass-burning and fossil-fuel emissions. These aerosol characteristics are consistent with MODIS observations showing enhanced fine-mode AOD over West and Southern Africa during peak biomass-burning seasons, reflecting intense fire activity and reduced wet scavenging processes (Adesina et al., 2016; Remer et al., 2020). Similarly, MERRA-2 reanalysis indicates that carbonaceous aerosols, including black carbon and organic carbon, contribute approximately 50–80% of total AOD in these regions, further confirming the predominance of combustion-derived particles (Randles et al., 2017). CALIPSO observations provide additional support by detecting elevated smoke layers at altitudes of approximately 1–3 km, confirming the presence of absorbing aerosols consistent with low SSA retrievals (Winker et al., 2013). Sites such as Mbita and Skukuza, characterized by substantial contributions from BC and mixed aerosols (MXD), exemplify the combined influence of regional biomass burning and anthropogenic emissions (Boiyo et al., 2018; Ranaivombola et al., 2023; Millet et al., 2022).

In contrast, low FMF values (<0.4–0.5) and high SSA values (>0.90) are characteristic of coarse-mode, weakly absorbing aerosols, primarily mineral dust. This aerosol regime is dominated by Saharan and Sahelian dust transport, which is often intensified during the Harmattan season (Schuster et al., 2016). MODIS captures these conditions through elevated AOD values over North and West Africa, while CALIPSO observations reveal dust layers between approximately 2 and 5 km altitude, indicative of long-range transport processes (Winker et al., 2013). Consistent with these observations, MERRA-2 attributes approximately 40–70% of total AOD in these regions to dust aerosols, supporting the identification of polluted dust (PD) regimes.

Intermediate FMF (∼0.4–0.7) and SSA (∼0.85–0.92) values correspond to mixed aerosol (MXD) conditions, reflecting complex interactions between natural and anthropogenic aerosol sources, including secondary aerosol formation, atmospheric aging, and aerosol mixing processes (Bergstrom et al., 2022). Such conditions are particularly prominent during transitional seasons, when meteorological factors favor both aerosol emissions and chemical processing. CALIPSO observations of vertically mixed aerosol layers, together with MERRA-2 simulations showing the coexistence of dust, sea salt, and carbonaceous aerosols, provide strong support for the identification of these mixed regimes. Likewise, coastal and urban-influenced sites such as Henties Bay and Saada exhibit polluted continental (PC) characteristics, with MODIS indicating moderate aerosol loading and MERRA-2 highlighting significant contributions from secondary aerosol species (Levy et al., 2013).

Overall, despite known limitations associated with MODIS retrievals over bright surfaces, CALIPSO's narrow spatial sampling, and the model-dependent nature of MERRA-2 products, the strong agreement among these independent datasets provides substantial validation of the FMF–SSA classification framework. The integration of ground-based observations, satellite retrievals, and reanalysis products offers a comprehensive and reliable approach for aerosol characterization and source attribution across Africa.

Unlike conventional univariate or threshold-based classification methods, the FMF–SSA framework simultaneously evaluates the coupled variability of aerosol microphysical and radiative properties, thereby enhancing discrimination among spectrally overlapping aerosol types. The framework effectively distinguishes combustion-derived aerosols, characterized by high FMF and low SSA values, from mineral dust aerosols, which exhibit low FMF and high SSA values, while also capturing intermediate mixed states. Consequently, this multivariate approach reduces classification ambiguity, improves aerosol source identification, and provides a more robust representation of seasonal aerosol variability across the African continent.

3.3. FMF versus AE

Fig. 4 illustrates the relationship between FMF_{500} and $AE_{440-870}$

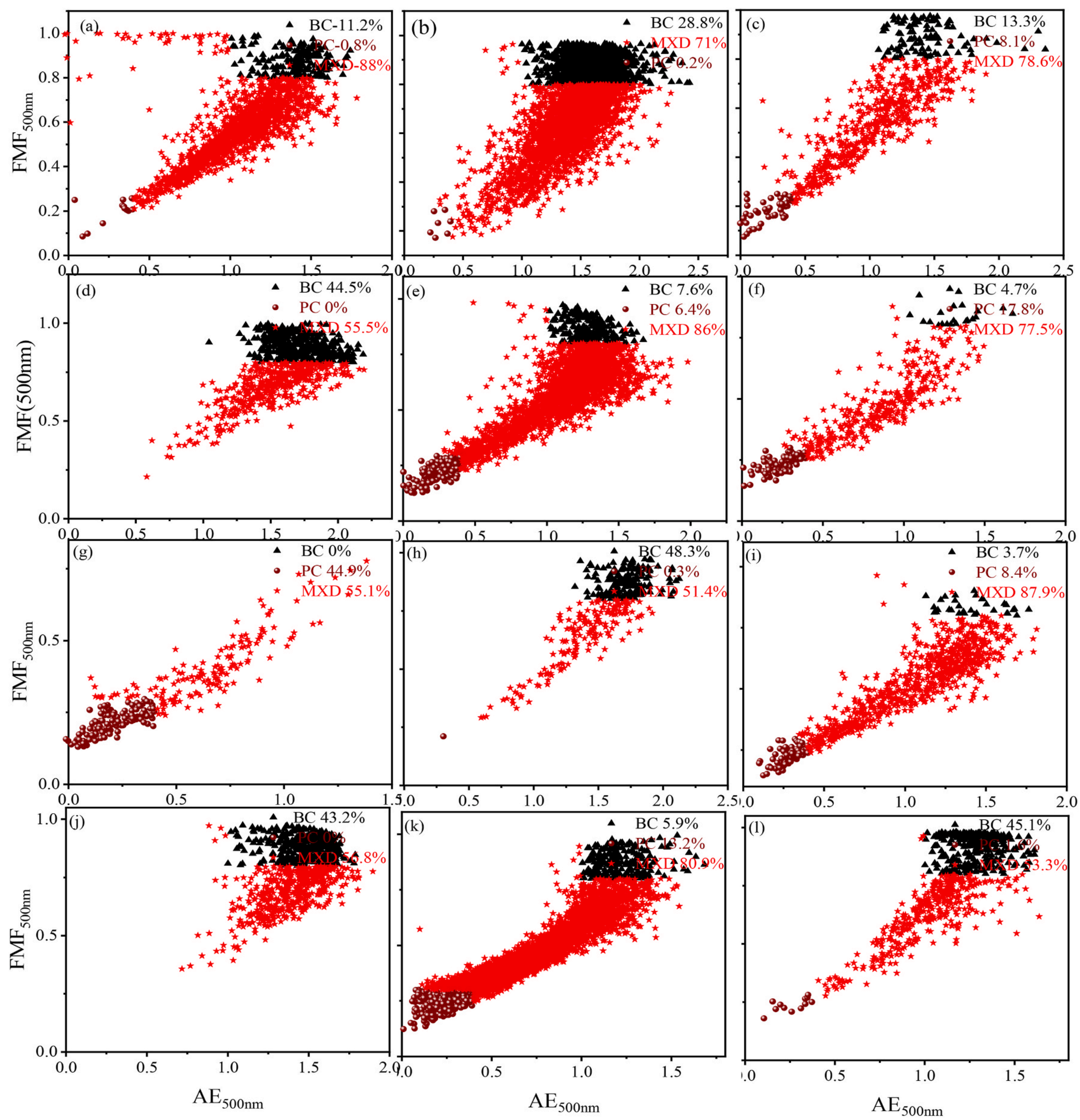

Fig. 4. Comparative analysis of FMF_{500} versus $AE_{440-870}$ across selected AERONET sites in Africa: (a) Mbita, (b) Skukuza, (c) Henties Bay, (d) MaunTower, (e) Cairo EMA-2, (f) Saada, (g) IER-Cinzana, (h) Gorongosa, (i) Tizi-Ouzou, (j) Bujumbura, (k) Ilorin, and (l) SEGC-Lope-Gabon. Aerosol types are classified as black carbon (BC), polluted continental (PC), and mixed aerosols (MXD).

across multiple AERONET sites in Africa, facilitating both inter-site comparisons and broader climatological interpretations of aerosol characteristics. The distribution of observations reveals three dominant aerosol regimes-black carbon (BC), mixed aerosols (MXD), and polluted continental aerosols (PC)-with distinct spatial variations linked to regional emission sources and atmospheric processes (Table 4). The Ångström exponent (AE), which is inversely related to particle size, indicates finer particles at higher values, whereas the fine-mode fraction (FMF) quantifies the relative contribution of fine-mode aerosols to the total aerosol population (Dubovik et al., 2002).

The aerosol patterns identified from the AE–FMF framework are strongly supported by satellite and reanalysis products, including MODIS, CALIPSO, and MERRA-2. In northern and arid regions, such as Cairo and Tizi-Ouzou, relatively low AE values and broadly distributed FMF values indicate the predominance of coarse-mode aerosols. These findings are consistent with MODIS observations showing elevated AOD over the Sahara and Sahel and with CALIPSO measurements revealing dust layers at altitudes between 2 and 5 km, indicative of long-range dust transport (Winker et al., 2013; Remer et al., 2020). MERRA-2 further corroborates these observations by attributing approximately 40–70% of total AOD in these regions to mineral dust aerosols (Randles et al., 2017).

In contrast, equatorial and tropical sites, including SEGC-Lope-Gabon and Gorongosa, exhibit high AE (>1.2) and FMF (>0.6) values, indicating the dominance of fine-mode aerosols associated with biomass burning and secondary aerosol formation. MODIS observations show moderate-to-high aerosol loading (AOD ~0.3–0.7) over these regions, while MERRA-2 attributes approximately 50–80% of total AOD to organic carbon and black carbon aerosols, consistent with combustion-related emission sources (Remer et al., 2020). CALIPSO observations of lofted smoke plumes between approximately 1 and 3 km altitude provide additional evidence for the vertical distribution of these fine-mode absorbing aerosols (Winker et al., 2013).

East African sites, such as Mbita, display intermediate AE and FMF values, indicative of mixed aerosol conditions. These observations are consistent with MERRA-2 simulations showing the coexistence of dust, carbonaceous aerosols, and secondary aerosol species, as well as CALIPSO observations of vertically mixed aerosol layers. Such transitional regimes highlight the complex interactions among local emissions, regional transport pathways, and atmospheric processing mechanisms. The identification of these intermediate aerosol states underscores the advantage of the AE–FMF framework in resolving transitional and mixed aerosol conditions that are often inadequately represented by conventional AOD–AE threshold-based classification approaches.

From a climatological perspective, the results reveal a pronounced north–south gradient in aerosol characteristics across Africa. Coarse, dust-dominated aerosols prevail over the arid regions of North Africa, whereas fine-mode, combustion-related aerosols dominate tropical and southern regions. Mixed aerosol regimes occupy intermediate environments, reflecting varying contributions from both natural and anthropogenic sources. The consistent representation of these patterns across AERONET, MODIS, CALIPSO, and MERRA-2 highlights the critical influence of regional climate, land-use practices, and emission dynamics on aerosol optical properties and their associated radiative effects. Collectively, the strong agreement among these independent observational and modeling datasets supports the interpretation that the AE–FMF framework functions as a physically constrained multivariate aerosol discrimination method rather than a purely descriptive threshold-based classification scheme.

Although several AERONET sites included in this study have relatively short observational records (4–5 years), which may not fully capture long-term interannual variability, this limitation does not substantially affect the primary conclusions. Aerosol classification was based on the intrinsic relationships among AOD–AE, FMF–SSA, and AE–FMF parameters rather than on frequency-based climatological statistics, making the methodology less sensitive to record length. Furthermore, the inclusion of multiple geographically distributed sites enables cross-validation of aerosol regimes across diverse environmental settings. Recurring seasonal aerosol patterns observed at these locations ensure that dominant source signatures and aerosol characteristics are adequately represented. Consequently, the results should be interpreted as representative of prevailing aerosol regimes rather than a complete long-term climatological assessment, thereby minimizing the influence of temporal data gaps.

Overall, the combined AE–FMF analysis provides a robust multivariate aerosol discrimination space in which particle-size characteristics and fine-mode aerosol contributions are evaluated simultaneously. This integrated approach reduces ambiguities associated with single-parameter analyses, improves aerosol source differentiation, and enhances the characterization of spatial and seasonal aerosol variability across the African continent.

4. Conclusions

This study investigated the spatial variability and classification of atmospheric aerosols across Africa using long-term AERONET observations from twelve representative sites spanning the period 1998–2024. A multivariate aerosol classification framework based on the relationships among aerosol optical depth (AOD), Ångström exponent (AE), fine-mode fraction (FMF), and single scattering albedo (SSA) was employed to characterize dominant aerosol regimes and evaluate their regional distributions. The key findings and contributions of this study are as follows:

1. The analysis revealed a pronounced spatial heterogeneity in aerosol regimes across Africa, with tropical sites dominated by mixed aerosols, reflecting the combined influence of biomass burning, urban emissions, and natural sources. This underscored the complexity of

Table 4
Percentage distribution (in %) of aerosol types obtained from different classification techniques across the selected AERONET sites.

Site	AE-AOD technique					FMF-SSA technique			FMF-AE technique		
	BUI	CCB	CMA	DDT	MXD	BC	MXD	PC	BC	MXD	PC
ICIPE Mbita	16.43	24.15	19.81	0.16	39.49	76.70	21.30	2	11.20	88	0.80
Skukuza	20.17	40.64	13.28	0.05	25.86	96.90	3.10	0	28.80	71	0.20
Henties Bay	23.37	60.00	1.78	0.00	14.85	96	0	4	13.30	78.60	8.10
Maun tower	23.37	60	1.78	0	14.85	100	0	0	44.50	55.50	0
Cairo EMA-2	43.38	3.23	4.47	3.27	45.65	11.90	42.90	45.20	7.60	86	6.40
Saada	1.02	14.29	46.43	4.08	34.18	10	65	25	4.70	77.50	7.80
IER Cinzana	1.80	1.08	21.51	19	56.63	1.30	31.20	67.50	0	55.10	44.90
Gorongosa	40.90	28.57	9.24	0	21.29	96	4	0	48.30	51.40	0.30
Tizi Ouzou	2.88	34.41	18.99	1.61	42.12	57	51.10	43.20	3.70	87.90	8.40
Ilorin	65.52	11.41	0.40	0.00	22.68	100	0	0	43.20	56.80	0
Bujumbura	16.48	4.84	1.48	29.63	47.57	15.80	67	17.20	5.90	80.90	13.20
SEGC-lope-Gabon	58.69	9.03	2.48	1.58	28.23	77.80	19.10	31	45.10	53.20	1.70

aerosol composition in these regions and the need for region-specific representation in climate models.

2. A clear latitudinal gradient was evident, where northern sites (e.g., Cairo and Tizi-Ouzou) were characterized by coarse-mode, dust-dominated aerosols, while equatorial and southern sites (e.g., SEGC-Lope-Gabon and Gorongosa) exhibited strong fine-mode dominance associated with biomass burning and secondary aerosol formation.
3. The integration of optical parameters demonstrated that absorbing aerosols are more prevalent in biomass burning regions, whereas scattering aerosols dominate in dust-influenced environments, indicating distinct regional radiative forcing regimes across the continent.
4. This study established a continent-wide comparative framework connecting aerosol optical properties with major sources and climatic zones, thereby enhancing understanding of aerosol-radiation interactions and contributing to the refinement of aerosol classification methods across Africa.

The aerosol classifications derived from AERONET observations were strongly supported by independent satellite and reanalysis datasets. The strong agreement among these datasets demonstrates the robustness and reliability of the proposed classification framework. Overall, the integration of AOD–AE, FMF–SSA, and AE–FMF relationships provides a physically constrained and comprehensive approach for aerosol discrimination across Africa. The multivariate framework reduces classification uncertainty, improves aerosol source attribution, and captures the complex interactions among dust transport, biomass burning, anthropogenic emissions, and atmospheric processing. These findings contribute to a better understanding of aerosol climatology over Africa and provide valuable observational constraints for climate models, air-quality assessments, and evaluations of aerosol radiative forcing. Future studies incorporating additional aerosol microphysical, chemical, and vertical profile measurements will further enhance aerosol characterization and improve assessments of aerosol–climate interactions across the continent. The relevance of this research to the Sustainable Development Goals (SDGs) is significant. For SDG 13 (Climate Action), detailed aerosol types contribute to climate modeling and understanding the impact of aerosol types on regional climate patterns.

Availability of data and materials

Data will be made available upon request. However, the data that support the findings of this study are available openly and can be downloaded freely at http://aeronet.gsfc.nasa.gov/.

Funding

This research did not receive any specific grant from funding agencies in the public, commercial, or non-profit sectors.

CRediT authorship contribution statement

Yonah Situma: Conceptualization, Data curation, Formal analysis, Investigation, Methodology, Visualization, Writing – original draft. **John W. Makokha:** Conceptualization, Investigation, Resources, Software, Supervision, Validation, Writing – review & editing. **Peter N. Khakina:** Data curation, Resources, Validation, Writing – review & editing. **Geoffrey W. Khamala:** Data curation, Methodology, Validation, Writing – review & editing. **Kanike Raghavendra Kumar:** Data curation, Methodology, Supervision, Validation, Writing – review & editing. **Richard Boiyo:** Conceptualization, Validation, Writing – review & editing.

Declaration of competing interest

The authors declare that they have no known competing financial interests or personal relationships that could have appeared to influence the work reported in this paper.

Acknowledgment

We owe our sincere thanks to all the Principal Investigators, Prof. Brent Holben, and his staff for establishing and maintaining the AERONET station, where the data is made available and used in this study. The lead author extends sincere gratitude to the Ministry of Higher Education, Science and Technology of Kenya and Kibabii University, Kenya, for providing an opportunity to undertake PhD studies. One of the authors (KRK) is grateful to the Department of Science and Technology (DST), Govt. of India, for awarding the SERB-SRG (Grant No. SRG/2020/001445), DST-FIST Level 1 (Grant No. SR/FST/PS-1/2018/35), and DST-PURSE (SR/PURSE/2023/196) schemes to the Department of Physics, KLEF. The authors would like to acknowledge the Editor-in-Chief of the Journal and the two anonymous reviewers for their fruitful comments and constructive suggestions towards improving the earlier version of the manuscript.

Data availability

Data will be made available on request.

References

Adesina, A.J., Kumar, K.R., Sivakumar, V., Piketh, S.J., 2016. Inter-comparison and assessment of long-term (2004–2013) multiple satellite aerosol products over two contrasting sites in South Africa. J. Atmos. Sol. Terr. Phys. 148, 82–95. https://doi.org/10.1016/j.jastp.2016.09.001.

Aklesso, Mangamana, Kumar, K. Raghavendra, Bu, Lingbing, Boiyo, Richard, 2018. Analysis of spatial-temporal heterogeneity in remotely sensed aerosol properties observed during 2005–2015 over three countries along the Gulf of Guinea Coast in Southern West Africa. Atmos. Environ. 182, 313–324.

Al-Thani, H., Koç, M., Isaifan, R.J., 2018. A review on the direct effect of particulate atmospheric pollution on materials and its mitigation for sustainable cities and societies. Environmental science and pollution research 25, 27839–27857.

Althaf, P., Kumar, K.R., Kannemadugu, H.B.S., 2024. Aerosol optical depth over the Andhra Pradesh State in South India from reanalysis data: spatiotemporal variabilities and machine learning approach. Earth Syst. Environ. 9 (4), 2797–2821. https://doi.org/10.1007/s41748-024-00465-2. https://link.springer.com/10.1007/s41748-024-00465-2. (Accessed 24 September 2024).

Althaf, P., Kumar, K.R., Kannemadugu, H.B.S., Berhane, S.A., Mahesh, B., 2025. Spatiotemporal variability of extinction coefficient of aerosols and their subtypes over Andhra Pradesh, South India from the CALIPSO Data. Earth Systems and Environment. https://doi.org/10.1007/s41748-025-00936-0. https://link.springer.com/10.1007/s41748-025-00936-0. (Accessed 26 November 2025).

Bergstrom, R.W., et al., 2022. Characterizing absorbing aerosols over Africa: an observational analysis using AERONET and satellite data. Atmos. Environ. 295, 119450. https://doi.org/10.1016/j.atmosenv.2022.119450.

Berhane, S.A., Althaf, P., Kumar, K.R., Bu, L., Yao, M., 2025. A comprehensive analysis of AOD and its species from reanalysis data over the Middle East and North Africa Regions: evaluation of model performance using machine learning techniques. Earth Syst. Environ. 9 (4), 3683–3708. https://doi.org/10.1007/s41748-024-00513-x. https://link.springer.com/10.1007/s41748-024-00513-x. (Accessed 5 November 2024).

Berhane, Samuel Abraham, Kumar, Kanike Raghavendra, Bu, Lingbing, 2024. A 13-year space-based climatological evolution of desert dust aerosols in the Middle East and North Africa regions observed by the CALIPSO. Sci. Total Environ. 948, 174793.

Bibi, H., Alam, K., Bibi, S., 2016. In-depth discrimination of aerosol types using multiple clustering techniques over four locations in Indo-Gangetic plains. Atmos. Res. 181, 106–114. https://doi.org/10.1016/j.atmosres.2016.06.017. https://linkinghub.elsevier.com/retrieve/pii/S0169809516301703.

Boiyo, R., Kumar, K.R., Zhao, T., 2017. Statistical intercomparison and validation of multisensory aerosol optical depth retrievals over three AERONET sites in Kenya, East Africa. Atmos. Res. 197, 277–288. https://doi.org/10.1016/j.atmosres.2017.07.012. https://linkinghub.elsevier.com/retrieve/pii/S0169809517303307.

Boiyo, R., Kumar, K.R., Zhao, T., 2018. Optical, microphysical and radiative properties of aerosols over a tropical rural site in Kenya, East Africa: source identification, modification and aerosol type discrimination. Atmos. Environ. 177, 234–252. https://doi.org/10.1016/j.atmosenv.2018.01.018.

Boiyo, Richard, Kumar, K. Raghavendra, Zhao, Tianliang, Guo, Jianping, 2019. A 10-year record of aerosol optical properties and radiative forcing over three environmentally

distinct AERONET sites in Kenya, East Africa. J. Geophys. Res. Atmos. 124 (3), 1596–1617.
Buchard, V., Randles, C.A., da Silva, A.M., et al., 2017. The MERRA-2 aerosol reanalysis, 1980 onward. J. Clim. 30 (17), 6823–6850.
Chaibou, A.A.S., Ma, X., Kumar, K.R., Jia, H., Tang, Y., et al., 2020. Evaluation of dust extinction and vertical profiles simulated by WRF-Chem with CALIPSO and AERONET over North Africa. J. Atmos. Sol. Terr. Phys. 199, 105213. https://doi.org/10.1016/j.jastp.2020.105213.
Chen, J., Li, C., Ristovski, Z., Milic, A., Gu, Y., Islam, M.S., Dumka, U.C., 2017. A review of biomass burning: emissions and impacts on air quality, health and climate in China. Sci. Total Environ. 579, 1000–1034.
Chin, M., Diehl, T., Dubovik, O., Eck, T.F., Holben, B.N., Sinyuk, A., Streets, D.G., 2014. Light absorption by pollution, dust, and biomass burning aerosols: a global model study and evaluation with AERONET measurements. Atmos. Chem. Phys. 14 (6), 3449–3467. https://doi.org/10.5194/acp-14-3449-2014.
Chung, C.E., Li, Z., Zhang, R., 2022. Aerosol impacts on climate and environment. Natl. Sci. Rev. 9 (4). https://doi.org/10.1093/nsr/nwac046 nwac046.
de Graaf, M., Tilstra, L.G., Aben, I., Stammes, P., 2010. Satellite observations of the seasonal cycles of absorbing aerosols in Africa related to the monsoon rainfall. Atmos. Environ. 4410, 1274–1283. https://doi.org/10.1016/j.atmosenv.2009.12.038.
Dubovik, O., Holben, B., Eck, T.F., Smirnov, A., Kaufman, Y.J., King, M.D., Slutsker, I., 2002. Variability of absorption and optical properties of key aerosol types observed in worldwide locations. J. Atmos. Sci. 59 (3), 590–608. https://doi.org/10.1175/1520-0469(2002)059<0590:VOAAOP>2.0.CO;2.
Eck, T.F., Holben, B.N., Reid, J.S., Dubovik, O., Smirnov, A., O'Neill, N.T., Slutsker, I., 2020. Analysis of aerosol optical properties and radiative forcing. J. Geophys. Res. Atmos. 125 (9). https://doi.org/10.1029/2020JD032467 e2020JD032467.
Filonchyk, M., Hurynovich, Volha, Yan, Haowen, Zhou, Liang, Gusev, Andrei, 2020. Climatology of aerosol optical depth over eastern Europe based on 19 years (2000–2018) MODIS TERRA data. Int. J. Climatol. 40 (7), 3531–3549. https://doi.org/10.1002/joc.6412.
Gauderman, W.J., Gilliland, G.F., Vora, H., Avol, E., Stram, D., et al., 2002. Association between air pollution and lung function growth in Southern California children: results from a second cohort. Am. J. Respir. Crit. Care Med. 166 (1), 76–84. https://doi.org/10.1164/rccm.2111021. https://academic.oup.com/ajrccm/article/166/1/76/8515854. (Accessed 1 July 2002).
Gobbi, G.P., Kaufman, Y.J., Koren, I., Eck, T.F., 2007. Classification of aerosol properties derived from AERONET direct sun data. Atmos. Chem. Phys. 7, 453–458.
Holben, B.N., Eck, T.F., Slutsker, I., Tanré, D., Buis, J.P., Setzer, A., Smirnov, A., 1998. AERONET— A federated instrument network and data archive for aerosol characterization. Remote Sensing of Environment 66 (1), 1–16.
Hsu, N.C., et al., 2023. MODIS aerosol product updates: a new approach for fine-mode fraction and SSA retrievals. Remote Sensing of Environment 303, 113094. https://doi.org/10.1016/j.rse.2023.113094.
Kanji, Z.A., Ladino, L.A., Wex, H., Boose, Y., Burkert-Kohn, M., Cziczo, D.J., Krämer, M., 2017. Overview of ice nucleating particles. Meteorol. Monogr. 58, 1.1–1.33.
Khamala, G.W., Makokha, J.W., Boiyo, R., Kumar, K.R., 2022. Long-term climatology and spatial trends of absorption, scattering and total aerosol optical depths over East Africa during 2001–2019. Environ. Sci. Pollut. Res. https://doi.org/10.1007/s11356-022-20022-6.
Khamala, G.W., Makokha, J.W., Wanyera, C., Kumar, K.R., Almazroui, M., et al., 2026. Vertical distribution of cloud area fraction and associated cloud radiative effects over East Africa using MERRA-2 reanalysis and CERES (2000–2025) Data. Earth Syst. Environ. https://doi.org/10.1007/s41748-026-01266-5. https://link.springer.com/10.1007/s41748-026-01266-5. (Accessed 15 June 2026).
Khamala, G.W., Makokha, J.W., 2025. Spatiotemporal variability and source apportionment of particulate matter (PM) emissions using binned size distributions: insights from MERRA-2 over Africa. Earth Syst. Environ. 2025. https://doi.org/10.1007/s41748-025-00641-y.
Khan, R., Kumar, K.R., Zhao, T., 2019. The climatology of aerosol optical thickness and radiative effects in Southeast Asia from 18-years of ground-based observations. Environ. Pollut. 254, 113025.
Khan, R., Kumar, K.R., Zhao, T., Ali, G., 2020. The contribution of different aerosol types to direct radiative forcing over distinct environments of Pakistan inferred from the AERONET data. Environ. Res. Lett. 15 (11), 114062.
Khan, Rehana, Kumar, Kanike Raghavendra, Zhao, Tianliang, Ullah, Waheed, de Leeuw, Gerrit, 2021. Interdecadal changes in aerosol optical depth over Pakistan based on the MERRA-2 reanalysis data during 1980–2018. Remote Sens. 13, 822.
Kim, Y.J., Kim, M.S., Lee, S.H., 2022. Improving discrimination between clouds and optically thick aerosols using a three-wavelength approach. Atmos. Meas. Tech. 15 (6), 3031–3045.
Kumar, K.R., Kang, Na, Yin, Yan, 2018. Classification of key aerosol types and their frequency distributions based on satellite remote sensing data at an industrially polluted city in the Yangtze River Delta, China. Int. J. Climatol. 38 (1), 320–336. https://doi.org/10.1002/joc.5178.
Levy, R.C., Remer, L.A., Mattoo, S., et al., 2013. The collection 6 MODIS aerosol products. Atmos. Meas. Tech. 6, 2989–3034.
Li, X.-Y., Wang, H., Chen, J., Endo, S., Kirschler, S., et al., 2023. Large-eddy simulations of marine boundary layer clouds associated with cold-air outbreaks during the ACTIVATE Campaign. Part II: Aerosol–meteorology–cloud interaction. J. Atmos. Sci. 80 (4), 1025–1045. https://doi.org/10.1175/jas-d-21-0324.1. https://journals.ametsoc.org/view/journals/atsc/80/4/JAS-D-21-0324.1.xml.
Logothetis, S.A., Salamalikis, Vasileios, Kazantzidis, Andreas, 2020. Aerosol classification in Europe, Middle East, North Africa and Arabian Peninsula based on AERONET version 3. Atmos. Res. 239, 104893. https://doi.org/10.1016/j.atmosres.2020.104893.
Makokha, J.W., Angeyo, H.K., Muthama, J.N., 2015. Sun-photometric study and multivariate analysis of aerosol optical depth variability over some representative sites of the Kenyan atmosphere. Int. J. Biochemiphys. 23 (15), 28.
Makokha, J.W., Kimani, J.N., Angeyo, H.K., Makokha, J.W., 2012. Estimation of radiative forcing due to aerosols over selected sites in Kenya. J. Meteorol. Relat. Sci. 6, 3–13.
Makokha, J.W., Masayi, N.N., Barasa, P., Ikoha, P.A., Konje, M.M., et al., 2024. Assessing the long-term changes in selected meteorological parameters over the North-Rift, Kenya: a regional climatology perspective. Hydrology 12 (3), 59–76.
Makokha, J.W., Odhiambo, J.O., Shem, J.G., 2018. Long-term assessment of aerosol radiative forcing over selected sites of East Africa. J. Geosci. Environ. Protect. 6 (4), 22.
Makokha, J.W., Angeyo, H.K., 2013. Investigation of radiative characteristics of the Kenyan atmosphere due to aerosols using sun spectrophotometry measurements and the COART model. Aerosol Air Qual. Res. 13 (1), 201–208.
Millet, T., Bencherif, H., Bounhir, A., Bègue, N., Lamy, K., Ranaivombola, M., Benkhaldoun, Z., Portafaix, T., Duflot, V., 2022. Aerosol distributions and transport over Southern Morocco from ground-based and satellite observations (2004–2020). Atmosphere 13, 923. https://doi.org/10.3390/atmos13060923.
Mishra, A.K., Gharai, B., Sharma, R., 2021. Biomass burning aerosols and their impacts on regional climate and air quality. Environ. Res. 195, 110785. https://doi.org/10.1016/j.envres.2021.110785.
Mukhopadhyay, S., Ningombam, S.S., Amoghavarsha, A.V., Madhavan, B.L., Eck, T.F., Dumka, U.C., Khatri, Pradeep, Gupta, Pawan, 2025. Classification of global aerosol types and its radiative effects using aerosol robotic network (AERONET) data. Atmos. Environ. 362, 121530. https://doi.org/10.1016/j.atmosenv.2025.121530.
Mulago, S.K., Makokha, J.W., Boiyo, R., 2024. Spatial-temporal variation of aerosol optical depth and ångström exponent over selected towns in Kenya: environmental impact and climate change. Open Access Library Journal 11 (7), 1–16.
Ngaina, J., Mutai, B., 2013. Observational evidence of climate change on extreme events over East Africa. Glob. Meteorol. 2 (2). https://doi.org/10.4081/gm.2013.e2.
Nguyen, H.T., et al., 2025. Aerosol characteristics and transport over southeast Asia. Atmos. Environ. https://doi.org/10.1016/j.atmosenv.2025.121530.
Nicolae, D., Vasilescu, J., Talianu, C., Binietoglou, I., Nicolae, V., et al., 2018. A neural network aerosol-typing algorithm based on lidar data. Atmos. Meas. Tech. 11 (10), 4137–4153.
O'Neill, N.T., Dubovik, O., Eck, T.F., 2001. Modified Ångström exponent for the characterization of submicrometer aerosols. Appl. Opt. 40 (15), 2368–2375. https://doi.org/10.1364/AO.40.002368.
Putaud, J.P., et al., 2021. Aerosol properties and variability across Europe. Atmos. Environ. https://doi.org/10.1016/j.atmosenv.2021.118237.
Ranaivombola, M., Bègue, N., Bencherif, H., Millet, T., Sivakumar, V., Duflot, V., Baron, A., Mbatha, N., Piketh, S., Formenti, P., et al., 2023. Aerosol optical properties and types over Southern Africa and Reunion island determined from ground-based and satellite observations over a 13-Year period (2008–2021). Remote Sens. 15, 1581. https://doi.org/10.3390/rs15061581.
Randles, C.A., da Silva, A.M., Buchard, V., et al., 2017. The MERRA-2 aerosol reanalysis. J. Clim. 30 (17), 6823–6850.
Ranjan, R., et al., 2024. Advancements in aerosol type discrimination using machine learning and multi-sensor data fusion. Atmos. Res. 295, 106895. https://doi.org/10.1016/j.atmosres.2023.106895.
Remer, L.A., Mattoo, S., Levy, R.C., Munchak, L.A., 2020. MODIS aerosol algorithm and products. Atmos. Meas. Tech. 13, 337–365.
Rupakheti, D., Kang, S., Rupakheti, M., Cong, Z., Panday, A.K., Chen, X., 2019. Aerosol optical depth (AOD): spatial and temporal variations and source identification over Central Asia. J. Environ. Sci. 76, 215–228.
Sangura, M.T., Althaf, P., Makokha, J.W., Boiyo, R., Kumar, K.R., 2025. Estimation and model performance of aerosol radiative forcing from radiative transfer models using the AERONET data over Kenya, East Africa. Adv. Space Res. 75 (1), 481–496.
Schuster, G.L., Dubovik, O., Holben, B.N., 2016. Angstrom exponent and bimodal aerosol size distributions. J. Geophys. Res.
Schuster, Gregory L., Dubovik, Oleg, Holben, Brent N., 2006. Angstrom exponent and bimodal aerosol size distributions. J. Geophys. Res. Atmos. 111 (D7), 2005JD006328. https://doi.org/10.1029/2005jd006328. https://agupubs.onlinelibrary.wiley.com/doi/10.1029/2005JD006328. (Accessed 14 April 2006).
Seinfeld, J.H., Pandis, S.N., 1998. Atmospheric Chemistry and Physics. John Wiley and Sons, New York.
Shaheen, Abdallah, Wu, Renguang, Aldabash, Midyan, 2020. Long-term AOD trend assessment over the Eastern Mediterranean region: a comparative study including a new merged aerosol product. Atmos. Environ. 238, 117736.
Shikwambana, L., Sivakumar, V., 2018. Investigation of aerosol characteristics and transport over South Africa using satellite, model simulations and LIDAR data. J. Atmos. Solar-Terres. Phy. 173, 150–159.
Shin, S.-K., Kim, J., Lee, J., Yoo, J.-W., Park, S.S., 2023. Dynamic regional aerosol models for satellite aerosol optical depth retrieval over East Asia. Atmos. Environ. 294, 119500. https://doi.org/10.1016/j.atmosenv.2022.119500.
Sicard, M., et al., 2020. Aerosol optical properties and climate interactions. Atmos. Res. https://doi.org/10.1016/j.atmosres.2020.104893.
Smirnov, A., Holben, B.N., Sayer, A.M., Giles, D.M., 2019. Marine aerosol optical depth properties derived from AERONET sites. Atmos. Chem. Phys. 19 (5), 3165–3181. https://doi.org/10.5194/acp-19-3165-2019.
Srivastava, A.K., Singh, S., Tiwari, S., Kanawade, V.P., 2014. Variability in atmospheric particulates and meteorological effects on its mass concentrations over Delhi, India.

Atmos. Res. 145, 45–56. https://doi.org/10.1016/j.atmosres.2014.03.023. https://linkinghub.elsevier.com/retrieve/pii/S0169809514001513.
Tang, T., Shindell, D., Samset, B.H., Boucher, O., Forster, P.M., et al., 2021. Distinct surface response to black carbon aerosols. Atmos. Chem. Phys. 21 (18), 13797–13809. https://doi.org/10.5194/acp-21-13797-2021. https://acp.copernicus.org/articles/21/13797/2021/.
Toledano, C., Cachorro, V.E., Berjon, A., De Frutos, A.M., Sorrribas, M., 2007. Optical depth and angsrom exponent climatology at EL aresosillo AERONENT site (Huelva, Spain). Q. J. R. Meteorol. Soc. 133, 795–807.
Wei, Jing, Li, Zhanqing, Bai, Kaixu, Zou, Linyun, Sun, Lin, Zhang, Wenhao, Peng, Yiran, Zhao, Shuhui, Zhou, Jingran, 2022. Spatially gap free analysis of aerosol type grids in China. ISPRS J. Photogram. Remote Sens. 193, 192–206.
Winker, D.M., Tackett, J.L., Getzewich, B.J., et al., 2013. CALIPSO aerosol vertical distribution. J. Clim. 26, 9929–9947.
Yu, X., Lü, R., Kumar, K.R., et al., 2016. Dust aerosol properties and radiative forcing observed in spring during 2001–2014 over urban Beijing, China. Environ. Sci. Pollut. Res. 23, 15432–15442. https://doi.org/10.1007/s11356-016-6727-9.
Zhang, X., et al., 2016. Aerosol pollution and optical characteristics over China. Environmental Pollution 218, 119–129. https://doi.org/10.1016/j.envpol.2015.12.021.